Geophys. J. Int. (2003) **153,** 497–507

A Holocene–Late Pleistocene geomagnetic inclination record from Grandfather Lake, SW Alaska

C. E. Geiss[1] and S. K. Banerjee[2]

[1]*Department of Physics, Trinity College,* 300 *Summit St, Hartford,* CT 06106, *USA. E-mail: christoph.geiss@trincoll.edu*
[2]*University of Minnesota,* 310 *Pillsbury Drive S.E., Minneapolis,* MN 55455-0219, *USA. E-mail: banerjee@umn.edu*

Accepted 2002 November 21. Received 2002 November 18; in original form 2002 August 5

SUMMARY

Our study of lake sediments from Grandfather Lake in SW Alaska (N59.8181°, W158.5597°) yields the first geomagnetic inclination record for Alaska that spans the entire Holocene. The record is based on three overlapping sets of piston cores and is well dated by seven AMS radiocarbon dates. Its magnetic component consists of PSD (5–15 μm) magnetite that occurs in concentrations ranging from 10 to 1000 ppm. Some samples may also contain titanomagnetite (TM30) as a minor component. Variations in the concentration of magnetic minerals are caused by changes in sediment source and organic productivity.

The magnetic inclination record shows several features between present and 15 ka BP, which shed light on the short-term behaviour of the geomagnetic field at high latitudes and can be used for site correlations. A distinct drop in inclination near 12 ka BP is a record of a possible local magnetic excursion.

Key words: Alaska, geomagnetic variation, Lake sediments, palaeomagnetism.

INTRODUCTION

Lake sediments can provide continuous, high-resolution records of palaeoenvironmental change, and their study is fundamental to our understanding of past and future continental climate change. In order to integrate local palaeorecords into regional or global climate reconstructions, however, it is necessary to accurately correlate them either by dating or by comparing common features found in all sites. Radiocarbon dating is often difficult in arctic sites owing to the scarcity of terrestrial macrofossils in tundra environments and the storage effects of soils and peatlands within the watershed (Abbott & Stafford 1996). Arctic lakes, however, can provide a climatic baseline for a region that is highly sensitive to even small changes in global climate and greatly impacted by present global warming trends. Since high-latitude peatlands presently store up to 460 Gt of carbon (Gorham 1991), small changes in arctic environments can have large feedback effects on the global climate system through the release of CO_2 into, or sequestering of CO_2 from the atmosphere (Oechel *et al.* 2000).

Short-term fluctuations of the Earth's magnetic field can be recorded in lake sediments and are a potential method for core correlations between regional sites. Geomagnetic secular variation is regionally consistent over the scale of several 100 km s^{-1}, and the amplitude of change is high at high latitudes owing to the proximity to the Earth's magnetic poles (Cox 1970).

Here we present a magnetic inclination record for Grandfather Lake in southwestern Alaska. The site is well dated by a series of AMS radiocarbon dates and is, to our knowledge, the only continuous palaeomagnetic record for Alaska that spans the last 15 ka.

METHODS

We obtained four cores from the deepest part of Grandfather Lake (water depth 20.15 m) using a modified Livingston piston corer (Wright 1967). Cores were retrieved in azimuthally unoriented, overlapping segments of 1 m length. The core segments were split lengthwise to be photographed and were described using visual inspection and smearslides. For magnetic analyses we subsampled the cores at approximately 2 cm resolution and placed the samples into weakly diamagnetic plastic boxes of 5.28 cm^3 volume.

Low-field magnetic susceptibility (κ) measurements were conducted on all samples using a Geofyzika Kappabridge, model KLY-2. We correlated the depths of all core segments based on the magnetic susceptibility data and sedimentary marker horizons (Fig. 1).

Our depth–age model (Fig. 2) is based on seven AMS ^{14}C dates. Dating was performed on wood fragments by the University of Arizona AMS facility, and all dates shown in this paper were calibrated using the software program CALIB (version 4.3, Stuiver & Reimer 1993; Stuiver *et al.* 1998). All dates are reported as calendar years before present. A summary of all dates is shown in Table 1.

Selected samples were subjected to stepwise alternating-field (AF) demagnetization up to a maximum field of 100 mT, and palaeomagnetic directions were obtained using the Linefind routine of the computer program Super IAPD (Kent *et al.* 1983). Anhysteretic remanent magnetization (ARM) was measured for a peak alternating field of 100 mT and a bias field of 50 μT. AF demagnetization and ARM acquisition were performed using a D-Tech D-2000 alternating field demagnetizer. Isothermal remanent magnetization

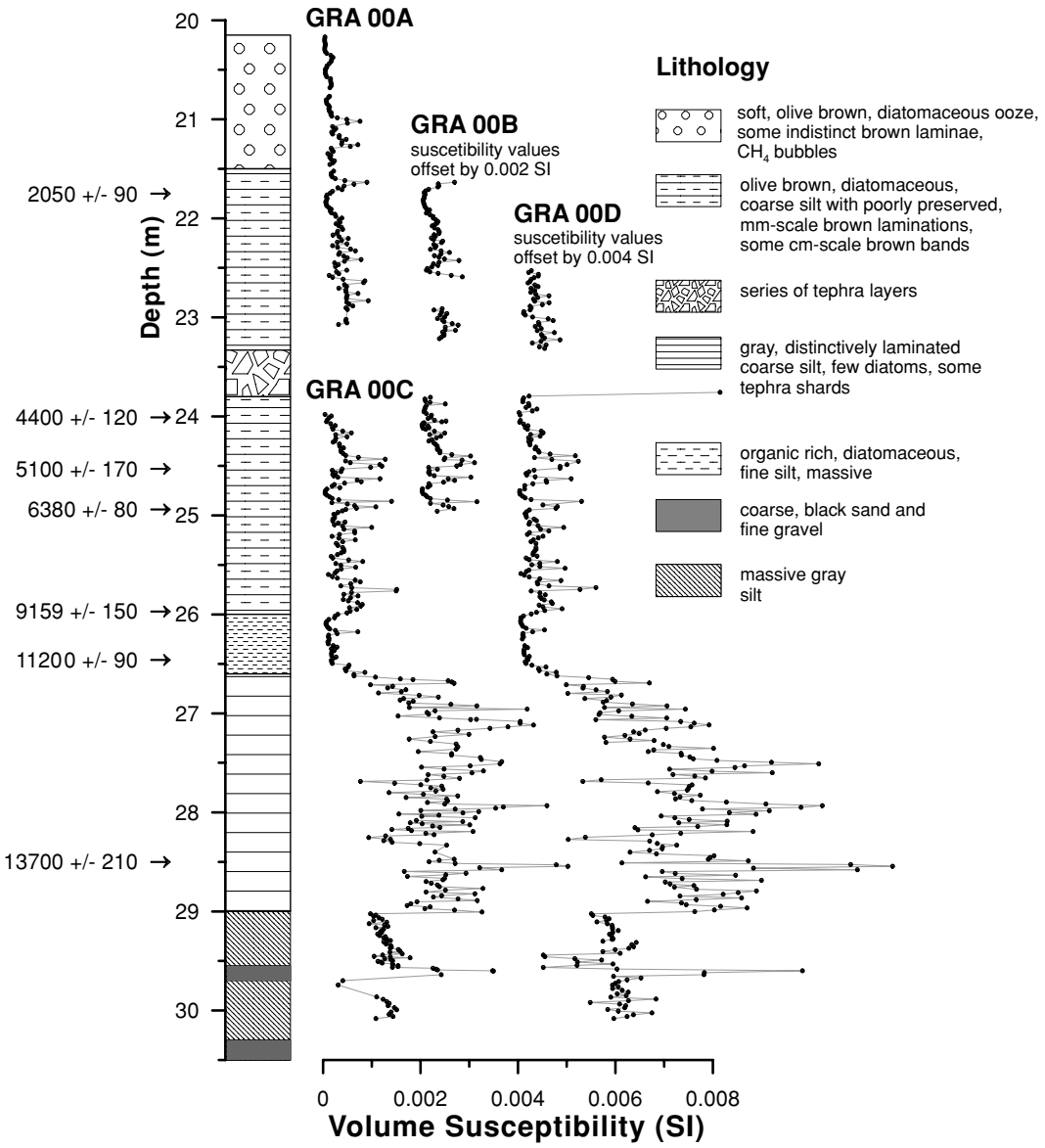

Figure 1. Volume susceptibility measurements for all samples from Grandfather Lake were used for depth correlation. Note that susceptibility values for GRA 00B and 00D are offset to the right by amounts indicated in the figure. The lithology is based on a visual inspection of the split cores and smearslide analyses. The locations of wood fragments used for radiocarbon analysis and their calibrated radiocarbon ages are indicated to the left of the depth axis. The depth is given in metres below the water surface.

(IRM_{100}) was acquired at 100 mT in the DC field of an electromagnet. All remanence parameters (NRM, ARM, IRM_{100}) were measured using a cryogenic magnetometer (2G Systems, model 760-R). Hysteresis parameters were measured in a maximum field of 1.3 T using a vibrating sample magnetometer (VSM), designed and constructed at the Institute for Rock Magnetism at the University of Minnesota, and a Princeton Measurement Corporation MicroMag Vibrating Sample Magnetometer (μVSM). Curie temperatures were obtained from $J_s(T)$ curves also measured on the μVSM. These measurements were conducted in a helium atmosphere to prevent chemical alteration. Thermal demagnetization of low-temperature IRM (with a magnetizing field of 2.5 T at 5 K) was performed in a Quantum Design MPMS 5 magnetic properties measurement system to observe magnetic phase transitions characteristic of magnetite and iron sulphides.

SITE DESCRIPTION

Grandfather Lake is a small glacial lake on the eastern side of the Wood-River mountains, approximately 90 km north of Dillingham, in southwestern Alaska (N59.8181°, W158.5597°). While most of the large glacial lakes in the area occupy bedrock basins (Mertie 1938), Grandfather Lake is dammed by a, now breached, terminal moraine and located on the eastern end of the area affected by Wisconsinan ice (Coulter *et al.* 1965). This interpretation is supported by a basal age of approximately 16 ka for Grandfather Lake sediments (Figs 2 and 6). The lake is fed by several small creeks and outflows via a small stream into Grant Lake, which is approximately 400 m to the south (Fig. 3). The site has been previously cored for palynological analyses by Hu *et al.* (1995), who also suggested the site for our magnetic study.

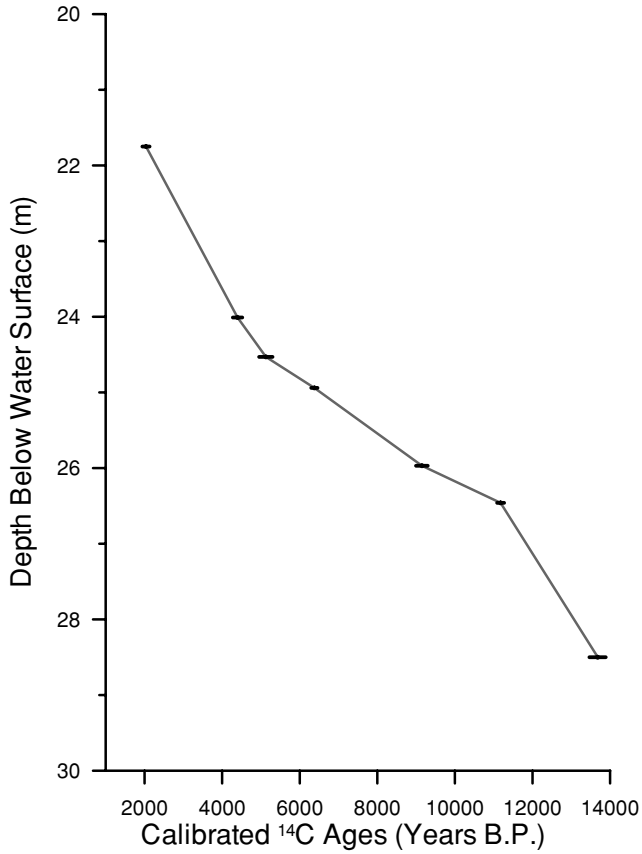

Figure 2. Depth–age curve for Grandfather Lake.

Holocene sediments consist of organic rich, olive brown to black diatomaceous ooze and coarse silt (20.15–26.00 m, see Fig. 1 for stratigraphic column). Diatom concentrations are variable but can reach up to 60 per cent, as estimated from smearslide analyses. The most recent sediments (20.15–21.5 m) are slightly disturbed by gas bubbles caused by methanogenesis. Often poorly preserved, millimetre-scale, dark-brown laminations are visible between 21.50 and 26.00 m depth. The Holocene sediments are interrupted by a tephra layer between 23.30 and 23.80 m depth. Tephra samples were not used for this study owing to problems of coring through this horizon and the resulting intense sediment deformation. A transition zone between 26.00 and 26.60 m consists of massive, olive-grey, coarse silt, which is followed by Late Pleistocene grey coarse silt and fine sand (26.60–29.00 m). These sediments are laminated, but preservation of the laminae is variable. The base of the core (>29.00 m) consists of massive, grey, coarse silt with interbedded black sand and fine gravel layers.

SEDIMENT–MAGNETIC CHARACTERIZATION

Magnetic mineralogy

Measurements of saturation magnetization (J_s) versus temperature reveal a magnetic phase with a Curie temperature of between 575 and 595 °C, indicating magnetite as the main magnetic mineral (Fig. 4). This interpretation is corroborated by thermal demagnetization curves of low-temperature SIRMs (Fig. 5), which all display well-developed Verwey transitions. In some Holocene samples J_s (T) curves reveal a second phase with a Curie temperature near 420 °C (Figs 4a and b), which is most probably caused by the presence of titanomagnetite (TM30). The magnetization of all samples increases when heated to 700 °C, which is either a result of the reduction of previously oxidized iron minerals, or the inversion of titanomagnetites into magnetite and a Ti-rich phase. No evidence for the presence of magnetic iron sulphides was found in $J_s(T)$ curves or any of the low-temperature measurements.

Concentration of magnetic minerals

The concentration of magnetic minerals has been estimated by measurements of saturation magnetization J_S (Fig. 6b). Assuming magnetite to be the main magnetic mineral, its concentration in the lake sediments varies between 10 and 1000 ppm. Concentrations up to 350 ppm occur in the tephra layer between 23.3 and 23.7 m, and yet unrecognized tephra may contribute to some of the high values of κ and J_S observed in the Late Pleistocene samples.

Values of all concentration-dependent parameters (κ, ARM, IRM, J_S) are high in sediments older than 11.2 ka, low for sediments deposited from 11.2 to 9.5 ka and variable, but generally low for the rest of the Holocene (Figs 6a and b).

Smearslide analyses reveal that organic productivity exerts a strong influence on the concentration of magnetic minerals with diatom concentrations as high as 60 per cent, diluting the terrigenous silt. Reductive dissolution of iron-oxides owing to organic matter decomposition may also influence the magnetic signal to some degree. The strongly magnetic sediments that were deposited during the Late Pleistocene contain a much greater abundance of coarse silt and fine sand with diatom concentrations generally below 10 per cent and organic material concentrated in a few dark brown layers. Tephra found throughout the core may also contribute to the magnetic signal; however, the resolution of our smearslide analysis is not high enough to allow for the quantification of tephra deposition through time.

Magnetic grain size

Hysteresis loops were measured for all samples used for palaeomagnetic investigations. None of the measured loops is wasp-waisted

Table 1. Summary of radiocarbon dating results.

Sample	Description	Lab. code	^{14}C age	2σ max (cal. ages) 2σ min
00B-15.5 cm	Wood	AA44383	2079 ± 40	2148 (2039, 2024, 2009) 1932
00D-71.0 cm	Wood	AA44385	3961 ± 45	4525 (4417) 4259
00C-50.0 cm	Wood	AA44384	4477 ± 60	5313 (5211, 5189, 5115, 5113, 5050) 4870
00C-95.0 cm	Wood	AA44381	5612 ± 50	6494 (6404, 6364, 6363) 6293
C-92.0 cm	Wood	AA44382	8164 ± 60	9398 (9125, 9113, 9087, 9047, 9032) 9005
C-40.7 cm	Wood	AA44380	9797 ± 60	11295 (11197) 11157
D-94.0 cm	Wood	AA44386	11739 ± 55	15139 (13809) 13453

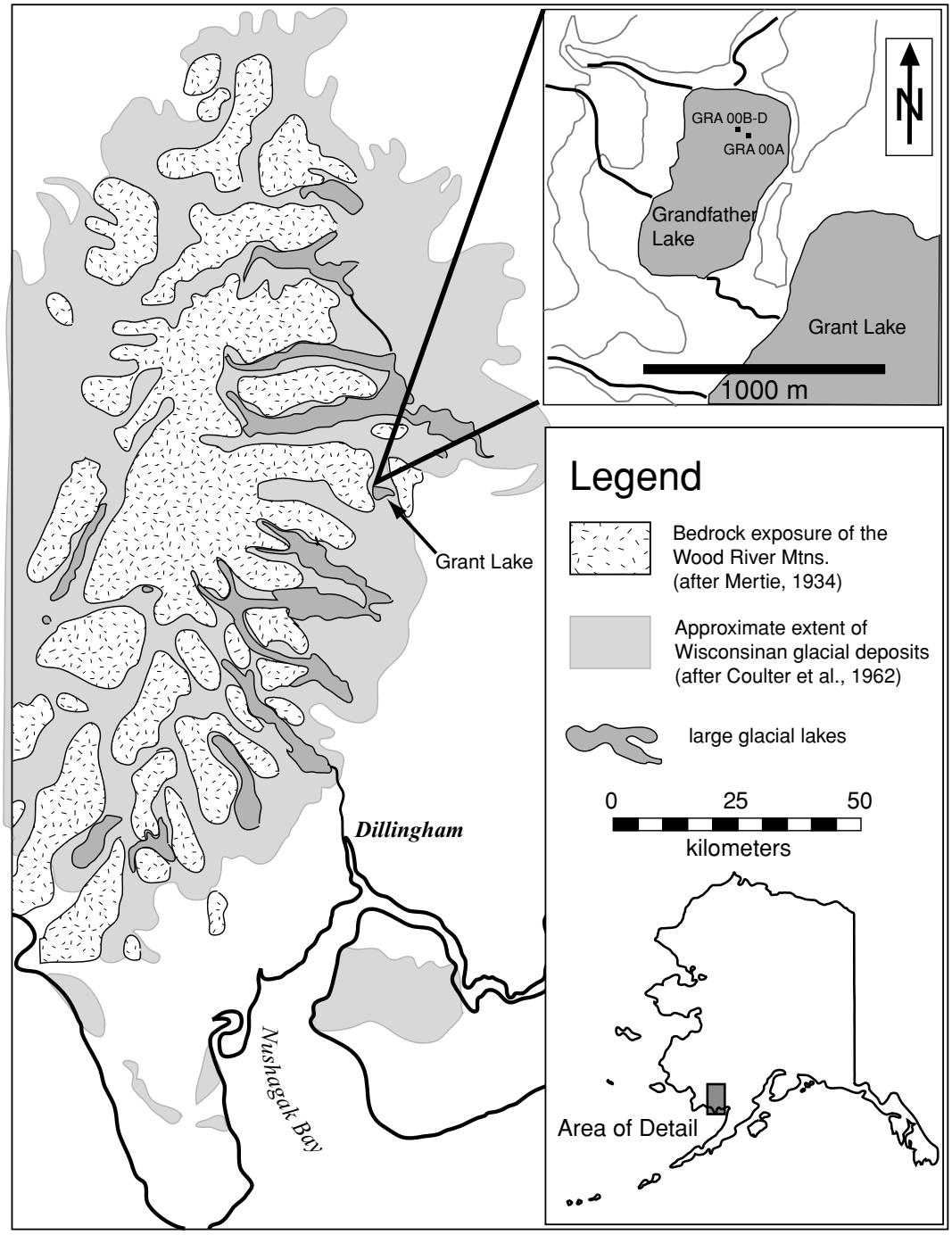

Figure 3. Generalized map of the Wood-River mountains, showing the location of Grandfather Lake and the extent of Wisconsinan age glacial sediments (after Coulter *et al.* 1965).

or pot-bellied, indicating that the magnetic component of the sediments is characterized by a simple coercivity distribution. All loops are further characterized by a strong paramagnetic component. On a graph of J_{rs}/J_S versus H_{cr}/H_c (Day *et al.* 1977) most samples plot towards the coarse end of the pseudo-single-domain (PSD) field (Fig. 7), suggesting bulk grain sizes between 5 and 15 μm (Dunlop 1981). A relatively coarse grain size distribution for most samples is confirmed by low ARM/IRM ratios between 1 and 5 per cent (Fig. 6c). With ARM being strongly dependent on grain interactions (Sugiura 1979), it is possible that the drop in ARM/IRM for strongly magnetic samples older than 11.2 ka is a result of concentration rather than grain size changes. To test this hypothesis we compared IRM acquisition and AF demagnetization curves for several representative samples (Cisowski 1981). All samples have crossover points (R values) between 0.27 and 0.25, indicating a significant, but more or less constant degree of grain interaction. Since R values are strictly valid only for single-domain particles we also measured ARM acquisition curves (Sugiura 1979) in bias

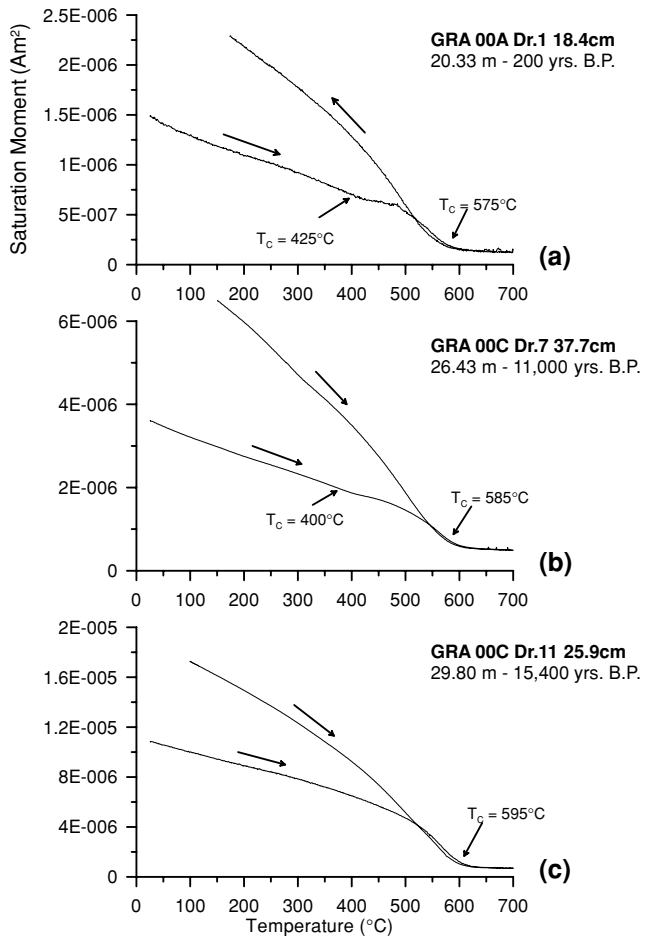

Figure 4. Temperature dependence of the saturation remanence J_S for three characteristic samples. The main Curie temperatures for all samples lie between 575 and 595 °C, which lies within the experimental error of the Curie temperature for magnetite (580 °C). Samples GRA 00A Dr1 18.4 cm and GRA 00C Dr7 37.7 cm show an additional inflection of the heating curve near 420 °C, indicating the presence of an additional titanomagnetite phase (TM30). Arrows denote heating and cooling curves.

fields up to 0.2 mT. These curves (not shown here) do not show any differences in grain interactions. Based on these analyses we interpret changes in ARM/IRM ratios as being primarily grain-size driven and conclude, in combination with the hysteresis data, that the magnetic component consists of coarse PSD magnetite.

On a graph of κ_{ARM} versus κ (Fig. 8, Banerjee *et al.* 1981) our samples fall into the fine-grained part of the diagram, contradicting our previous interpretation. Fig. 8, however, was calibrated using synthetic samples of relatively high magnetite concentrations. As pointed out by Tauxe (1993), these high concentrations are likely to lead to grain interactions, thus lowering κ_{ARM} and making it dependent on the bias-field used during ARM acquisition, and underestimating particle size. Imperfect dispersion or clumping of the magnetite component may further increase this effect.

PALAEOMAGNETIC RESULTS

Directional record

Vector endpoint plots and demagnetization curves (Fig. 9) show that the natural remanent magnetization (NRM) signal is demagnetized in alternating fields smaller than 100 mT. This is consistent with the results from rock-magnetic investigations, which identified coarse PSD magnetite as the carrier of the magnetic signal. Many samples show a small viscous overprint, acquired during several months of storage, which was easily removed in a 10 mT field. All samples yielded stable palaeomagnetic directions with maximum angular deviations (MAD angles) generally below 3°. The entire data set (Fig. 6d), however, shows moderate scatter, which is probably caused by slight orientation errors and deformation of the soft sediments arising from methanogenesis and subsampling for magnetic analyses.

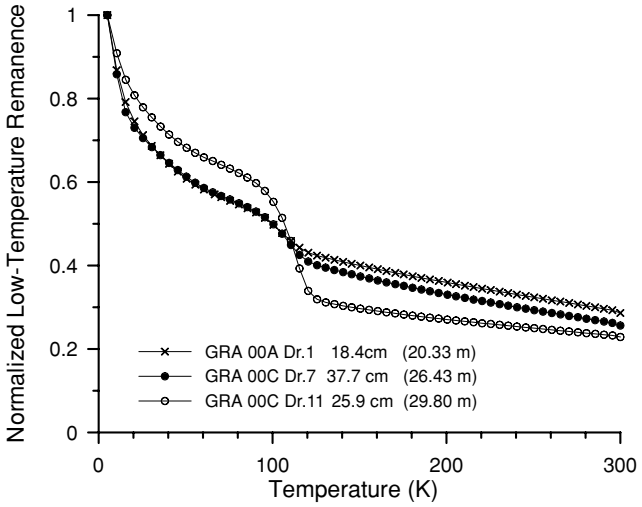

Figure 5. Thermal demagnetization of saturation remanence given at 5 K in a magnetizing field of 2.5 T. Drops in remanence near 120 K are caused by the Verwey transition of magnetite.

Since our cores are azimuthally unoriented we did not attempt to reconstruct variations in magnetic declination. With inclination values as high as 88° the error in the horizontal component was often too high to reorient the relatively short core segments (1 m length) into a robust declination record.

Fig. 6(d) shows the magnetic inclination record for Grandfather Lake. The dashed line represents the expected inclination of 73.8° for a site at 51.8° latitude. The record was compiled using samples from all four sites. The individual scatter is caused by local disturbances, such as soft sediment deformation, which is especially severe in the topmost part of the core, where CH_4-degassing during and after coring created large bubbles in the extremely soft sediments. The combined record (solid line), however, displays distinct large-scale features, such as the inclination lows between 2.5–3.5 and 11.5–12.5 ka, or the high inclinations at 6.5 and 10 ka. These features may be used for regional core correlations and can aid in the age control of sediment cores that cannot be dated otherwise.

Comparison with other North American records

The magnitude and rate of change of secular variation recorded at Grandfather Lake are similar to the record observed by Verosub (1982) for Tangle Lakes. However, there is no local palaeomagnetic record of comparable length and resolution that would allow us to validate our observed regional secular variation curve. Fig. 10 shows a comparison of the Grandfather Lake inclination record with two long, well-dated, high-resolution records from North America.

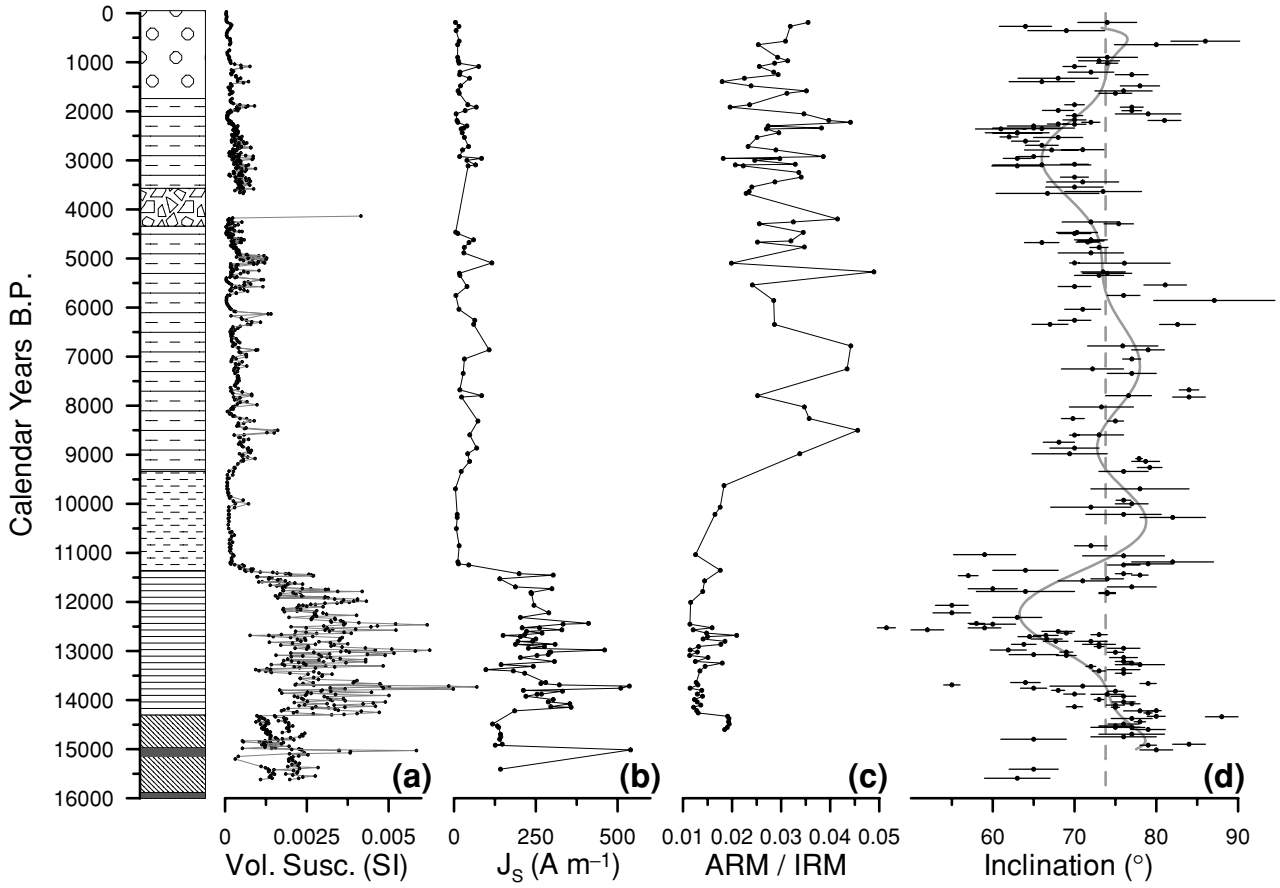

Figure 6. Sediment-magnetic parameters and the inclination record for Grandfather Lake. (a) Magnetic susceptibility κ and (b) saturation magnetization J_S are proxies for the concentration of magnetic minerals, (c) the ratio of ARM/IRM is interpreted as a grain size proxy, with higher ratios indicating a relative increase in the abundance of fine-grained SD particles. (d) The inclination record is based on samples from all four sites. Error bars denote the MAD angle. The legend for lithology can be found in Fig. 1.

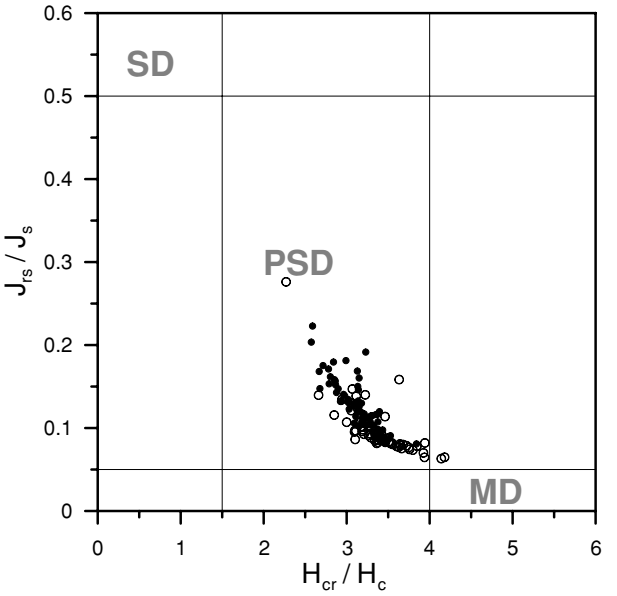

Figure 7. Hysteresis parameters for the Holocene (solid symbols) and the Late Pleistocene (open symbols). All samples fall into the coarse end of the pseudo-single-domain field.

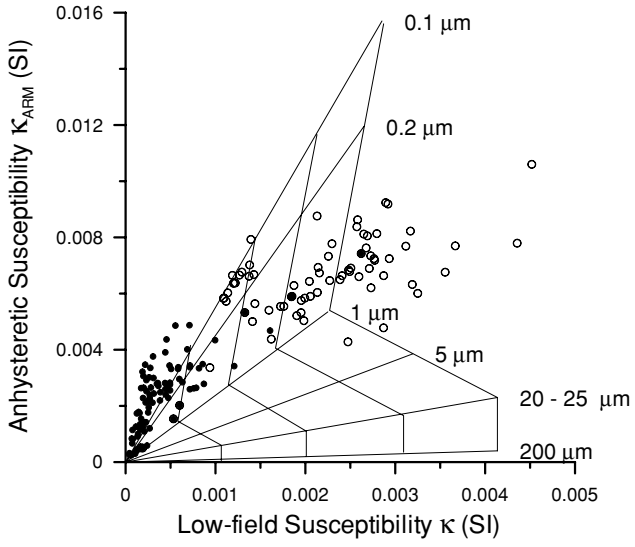

Figure 8. Plot of anhysteretic susceptibility κ_{ARM} versus low-field susceptibility κ. Grain-size contours are based on measurements of synthetic samples by Banerjee *et al.* (1981). For more information see the text. Solid symbols, Holocene samples; open symbols, Late Pleistocene samples.

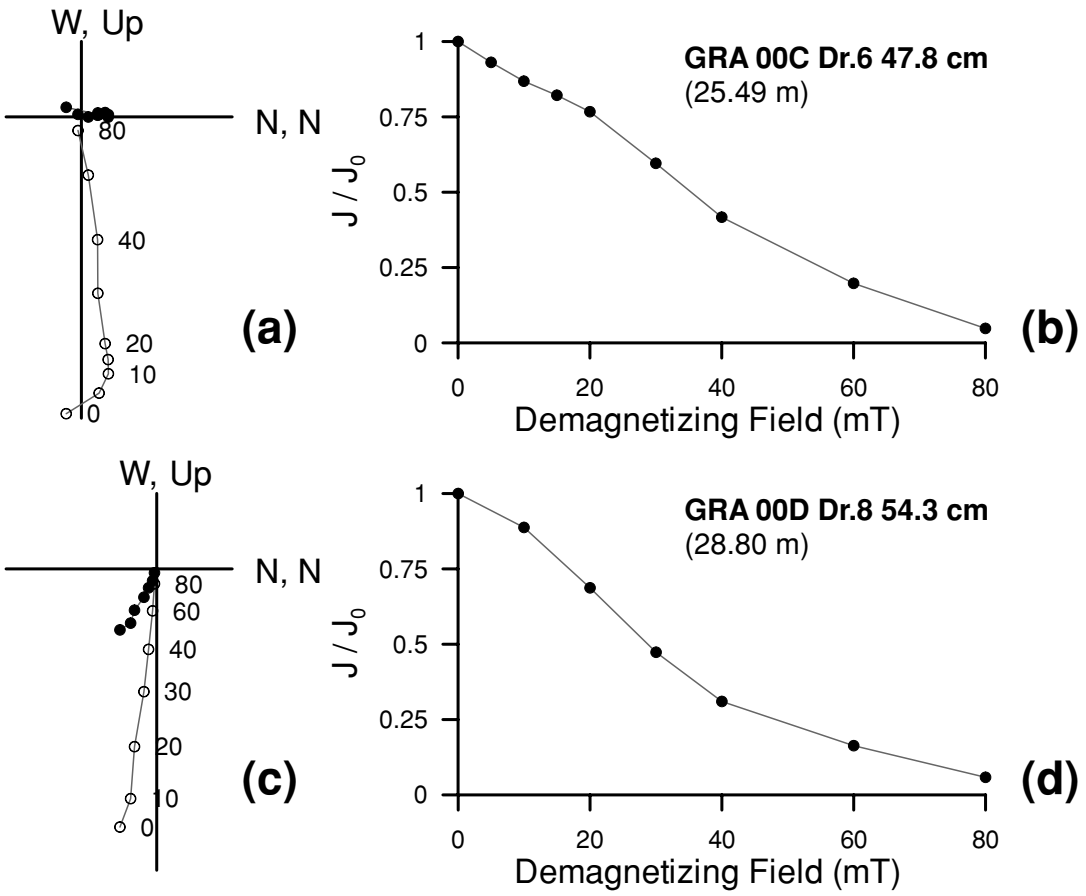

Figure 9. Demagnetization behaviour for two characteristic samples. (a), (c) Orthogonal projections of the NRM vector show changes in orientation and intensity of the NRM signal during stepwise alternating field demagnetization (Zijderveld 1967). Solid symbols represent projections on to the horizontal plane. Open symbols show projection on to vertical N–S plane. Labels indicate the magnitude of the demagnetizing field. (b), (d) Graphs showing the decreasing NRM intensity during AF demagnetization.

The palaeomagnetic record from Elk Lake, Minnesota (Sprowl & Banerjee 1989) is dated by a series of radiocarbon analyses and counting of annual laminations (Sprowl 1993). A tephra chronology and radiocarbon dates provide the age control for the Fish Lake, Oregon, palaeomagnetic record (Verosub *et al.* 1986).

Even though the three sites are spaced several thousand kilometres apart it is possible to correlate several large-scale features across the records. The inclination low between 2500 and 5000 yr BP is present in Fish Lake (2500–4200 yr BP) and Elk Lake (1200–5000 yr BP). Several inclination lows of shorter duration can also be correlated between all three sites as shown in Fig. 10. The drop in inclination at the base of the Fish Lake record has been attributed to inclination shallowing in the early, post-glacial deposits. At Grandfather Lake the sedimentary record extends further back in time and a similar drop in inclination occurs in glacial silts approximately 3 m above the basal sand and gravel, possibly recording a local magnetic excursion. The absence of sedimentological changes and high inclination values above and below the event make inclination shallowing an unlikely cause for the observed feature. In Sweden a contested excursion, the Gothenburg 'flip', has also been claimed at this time period (Morner & Lanser 1974), but has not been identified in lacustrine records from Minnesota (Banerjee *et al.* 1979). Additional studies of long lacustrine records from Alaska will be necessary to decide whether the event is a regional feature, or whether the observed inclination low is an artefact caused by sedimentological or diagenetic processes as claimed by Verosub *et al.* (1986) and Snowball (1997), respectively.

Relative palaeointensity

To successfully use variations in normalized NRM (e.g. NRM/ARM or NRM/κ) for the reconstruction of past changes in geomagnetic field intensity it is necessary that sediments pass several rock-magnetic criteria as outlined by King *et al.* (1983) and Tauxe (1993). Sediment samples best suited for relative palaeointensity reconstructions have a magnetic carrier that consists largely of (titano)magnetite with a grain size distribution between 1 and 15 μm in order to minimize the effects of magnetic mineralogy and grain size on the remanence acquisition process. Since ARM is particularly sensitive to grain interactions, the concentration of magnetic minerals should not vary by more than a factor of 10–20. The resulting palaeointensity record should also show little correlation with lithology and sediment-magnetic signal (Tauxe & Wu 1990).

Our rock-magnetic investigations show that the magnetic signal is carried by magnetite of the appropriate grain size. The differences in magnetic concentration between Holocene and Pleistocene samples, however, vary by more than two orders of magnitude. Fig. 11 shows the coercivity spectra for NRM, ARM and IRM_{100} for a characteristic sample. It is apparent that NRM is carried by a mixture of coarse and fine grains and neither ARM nor IRM_{100} are

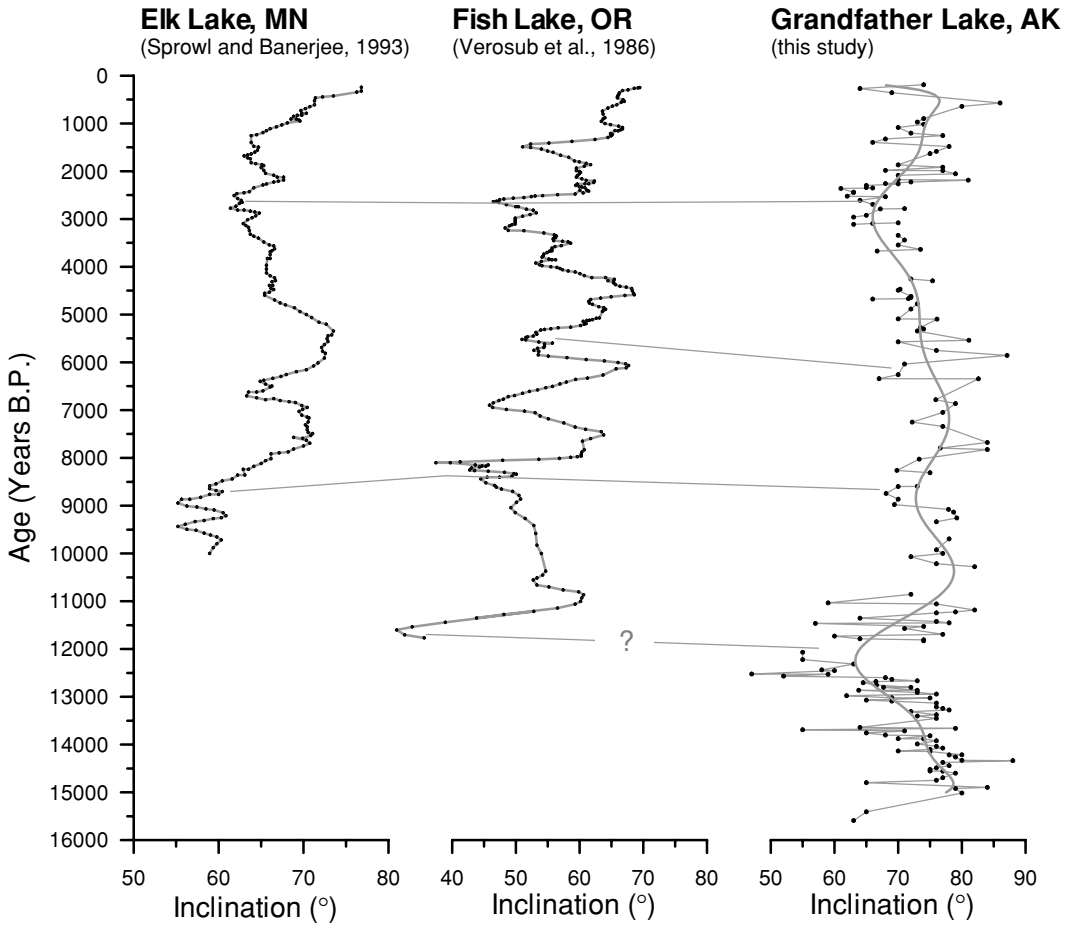

Figure 10. Comparison of the Grandfather Lake magnetic inclination record with other long lacustrine records from North America.

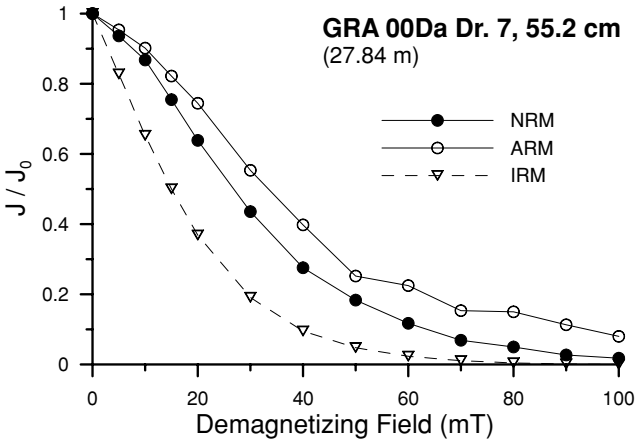

Figure 11. Demagnetization curves for NRM, ARM and IRM for sample GRA 00Da Dr7 55.2 cm.

perfect normalizers for relative palaeointensity reconstructions (Levi & Banerjee 1976). In Fig. 12 we therefore compare three potential proxies of relative palaeointensity: NRM/ARM, NRM/IRM_{100} and NRM/κ. The three proxies show some similarities, but a comparison with variations in κ and ARM/IRM (Figs 11d and e) shows that all palaeointensity records reflect to at least some degree changes in magnetic concentration and grain size. Scatter plots of reconstructed palaeointensity versus magnetic susceptibility confirm significant correlation between NRM/ARM and sediment-magnetic parameters (Figs 13a and b). The ratio of NRM/κ is less dependent on concentration changes (Fig. 13c), but shows some correlation with grain size for higher values of ARM/IRM (Fig. 13d). Cross-correlation analyses (not shown here) confirm the qualitative results obtained from Fig. 13 by indicating significant correlation between palaeointensity reconstructions and the underlying sediment-magnetic signal.

Given the high variability in magnetite concentration and grain size, it is not surprising that Grandfather Lake does not yield a robust palaeointensity record. Even during the Holocene (closed symbols in Fig. 13), when samples contain less magnetite and satisfy the criteria of uniformity laid out by King *et al.* (1983) and Tauxe (1993), there is a strong correlation between magnetic concentration and grain size, with strongly magnetic samples being coarser grained. The shift to coarser grain sizes expresses itself in both higher ARM/IRM and J_{rs}/J_S ratios. At present we do not know the causes of these variations, which may contain a valuable palaeoclimatic signal, but they turn Grandfather Lake sediments into poor recorders of geomagnetic field intensity.

CONCLUSIONS

(1) Our cores from Grandfather Lake, SW Alaska provide a continuous, well-dated record that spans the last 15 ka.

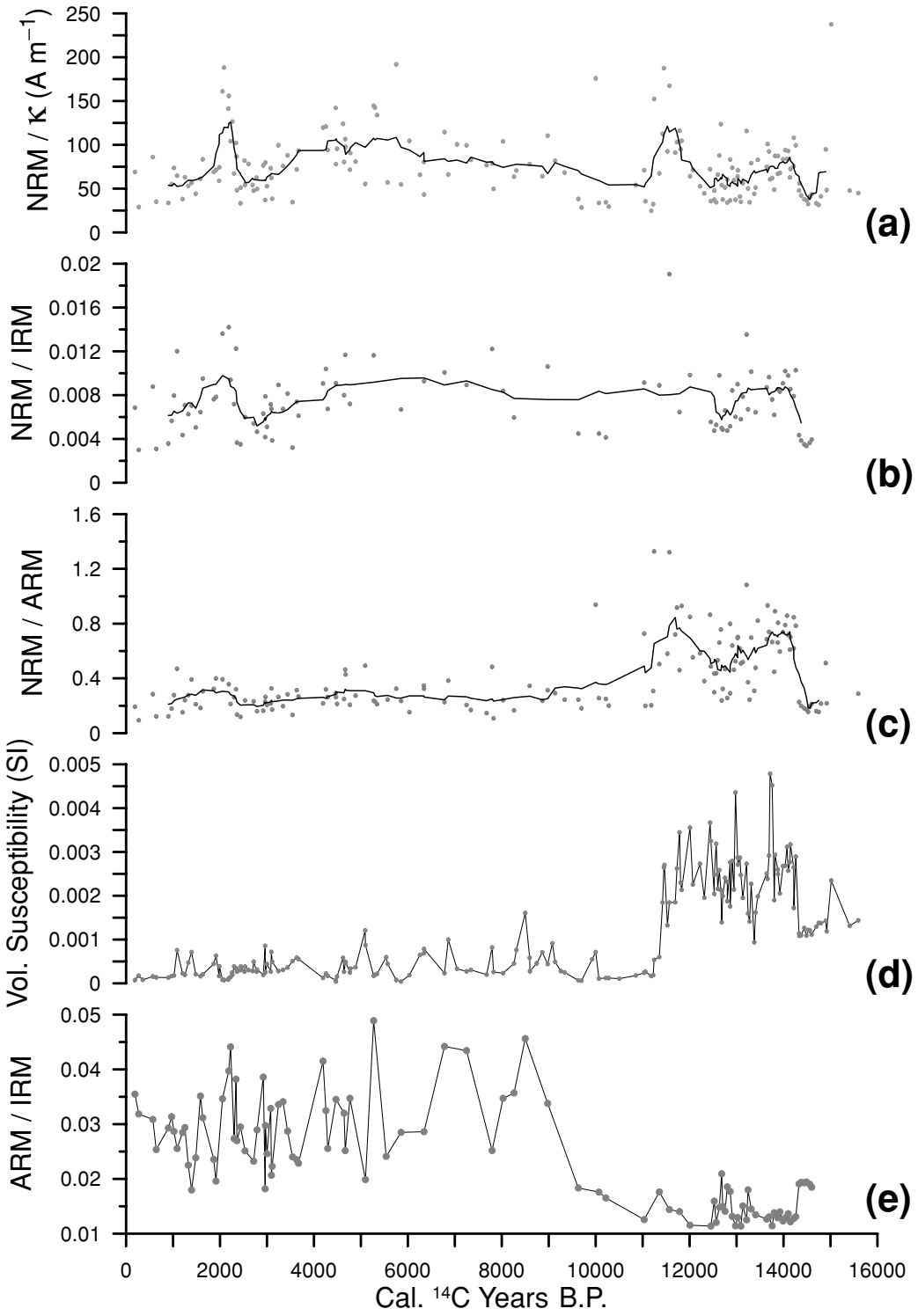

Figure 12. (a)–(c) Reconstructions of geomagnetic palaeointensity using various normalizing parameters for NRM. (d), (e) For comparison magnetic susceptibility (concentration proxy) and ARM/IRM (grain size proxy) are also shown.

(2) The main magnetic component consists of coarse-PSD magnetite. Some samples also contain a minor component of titanomagnetite (TM30), and we found no evidence of ferrimagnetic iron sulphides.

(3) Magnetite concentrations range from 10 to 1000 ppm and are controlled by organic productivity changes, with diamagnetic diatoms and organic matter diluting highly magnetic, terrigenous silt and fine sand.

(4) Owing to the non-uniform sediments we were unable to reconstruct a reliable palaeointensity record for this high-latitude site.

(5) The magnetic inclination record, however, shows robust, large-scale features that may be used for regional correlations with otherwise undated sites.

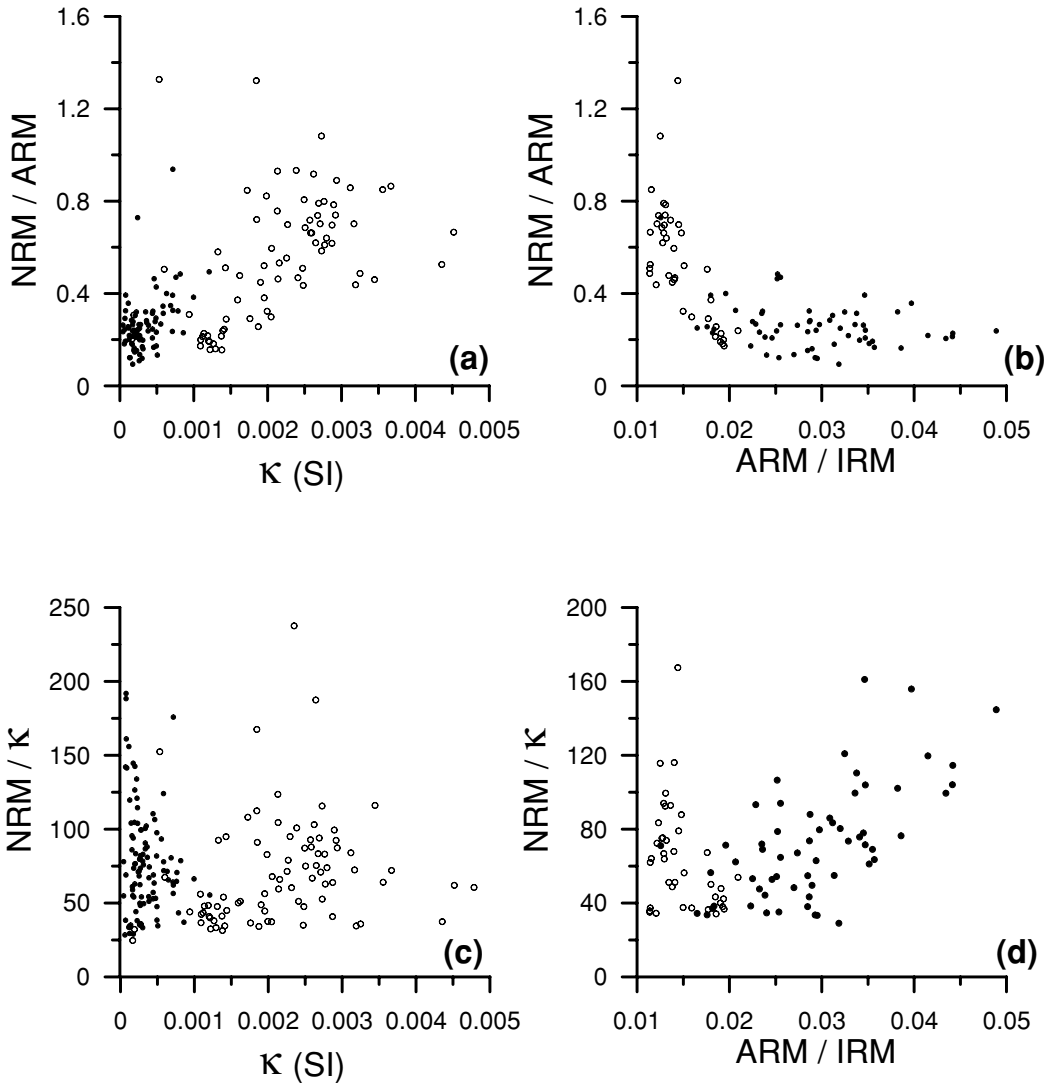

Figure 13. Scatter plots of (a) NRM/ARM versus magnetic susceptibility κ, (b) NRM/ARM versus ARM/IRM, (c) NRM/κ versus κ and (d) NRM/κ versus ARM/IRM to show correlations between palaeointensity proxies and underlying sediment-magnetic parameters. Solid symbols denote Holocene, open symbols denote Late Pleistocene samples.

ACKNOWLEDGMENTS

We are grateful to J. Dorale and L. Urbano for coring assistance, F.S. Hu for advice on site selection and logistical support in the field and M. Jackson for helpful discussions during this project. All magnetic analyses were performed at the Institute of Rock Magnetism, which is funded by the W.M. Keck Foundation, the National Science Foundation's Earth Science Division's Instrumentation and Facilities Programme and the University of Minnesota. Valuable comments by D. Stone and an anonymous reviewer helped to improve the manuscript. The study was supported by NSF grant 9809150. This is IRM publication 0203.

REFERENCES

Abbott, M.B. & Stafford, T.W., Jr, 1996. Radiocarbon geochemistry of modern and ancient arctic lake systems, Baffin Island, Canada, *Quat. Res.,* **45,** 300–311.

Banerjee, S.K., Lund, S.P. & Levi, S., 1979. Geomagnetic record in Minnesota lake sediments—absence of the Gothenburg and Erieau excursions, *Geology,* **7,** 588–591.

Banerjee, S.K., King, J. & Marvin, J., 1981. A rapid method for magnetic granulometry with applications to environmental studies, *Geophys. Res. Lett.,* **8,** 333–336.

Cisowski, S., 1981. Interacting vs. non-interacting single domain behavior in natural and synthetic samples, *Phys. Earth planet. Inter.,* **26,** 56–62.

Coulter, H.W., Hopkins, D.M., Karlstrom, T.N.V., Pewe, T.L., Wahrhaftig, C. & Williams, J.R., 1965. Map showing the extent of glaciations in Alaska, I-415, US Geological Survey, Washington, DC.

Cox, A., 1970. Latitude dependence of the angular dispersion of the geomagnetic field, *Geophys. J. R. astr. Soc.,* **20,** 253–269.

Day, R., Fuller, M. & Schmidt, V.A., 1977. Hysteresis properties of titanomagnetites: grain-size and compositional dependence, *Phys. Earth planet. Inter.,* **13,** 260–267.

Dunlop, D.J., 1981. The rock magnetism of fine particles, *Phys. Earth planet. Inter.,* **26,** 1–26.

Gorham, E., 1991. Northern peatlands: role in the carbon cycle and probable responses to climatic warming, *Ecol. Appl.,* **1,** 182–195.

Hu, F.S., Brubaker, L.B. & Anderson, P.M., 1995. Postglacial vegetation and climate change in the northern Bristol Bay region, southwestern Alaska, *Quat. Res.,* **43,** 382–392.

Kent, J.T., Briden, J.C. & Mardia, K.V., 1983. Linear and planar structure in ordered multivariate data as applied to progressive demagnetization of paleomagnetic remanence, *Geophys. J. R. astr. Soc.,* **75,** 593–621.

King, J.W., Banerjee, S.K. & Marvin, J., 1983. A new rock-magnetic approach to selecting sediments for geomagnetic paleointensity studies: application to paleointensity for the last 4000 years, *J. geophys. Res.,* **88,** 5911–5921.

Levi, S. & Banerjee, S.K., 1976. On the possibility of obtaining relative paleointensities from lake sediments, *Earth planet. Sci. Lett.,* **29,** 219–226.

Mertie, J.B., Jr, 1938. The Nushagak District, Alaska, *USGS Bull.,* **903,** 96.

Morner, N.A. & Lanser, J.P., 1974. The Gothenburg magnetic 'flip', *Nature,* **251,** 408–409.

Oechel, W.C., Vourlitis, G.L., Hastings, S.J., Zulueta, R.C., Hinzman, L. & Douglas, K., 2000. Acclimation of ecosystem CO_2 exchange in the Alaskan Arctic in response to decadal climate warming, *Nature,* **406,** 978–981.

Snowball, I.F., 1997. Gyroremanent magnetization and the magnetic properties of greigite-bearing clays in southern Sweden, *Geophys. J. Int.,* **129,** 624–636.

Sprowl, D.R., 1993. On the precision of the Elk Lake varve chronology, *Geol. Soc. Am. Special Paper,* **276,** 69–74.

Sprowl, D.R. & Banerjee, S.K., 1989. The Holocene paleosecular variation record from Elk Lake, Minnesota, *J. geophys. Res.,* **94,** 9369–9388.

Stuiver, M. & Reimer, P.J., 1993. Extended ^{14}C database and revised CALIB radiocarbon calibration program, *Radiocarbon,* **35,** 215–230.

Stuiver, M., Reimer, P.J. & Braziunas, T.F., 1998. High-precision radiocarbon age calibration for terrestrial and marine samples, *Radiocarbon,* **40,** 1127–1151.

Sugiura, N., 1979. ARM, TRM and magnetic interactions: concentration dependence, *Earth planet. Sci. Lett.,* **42,** 451–455.

Tauxe, L., 1993. Sedimentary records of relative paleointensity of the geomagnetic field: theory and practice, *Rev. Geophys.,* **31,** 319–354.

Tauxe, L. & Wu, G., 1990. Normalized remanence in sediments of the western equatorial Pacific: relative paleointensity of the geomagnetic field?, *J. geophys. Res.,* **95,** 12 337–12 350.

Verosub, K.L., 1982. A paleomagnetic record from Tangle Lakes, Alaska: large amplitude secular variation at high latitudes, *Geophys. Res. Lett.,* **9,** 823–826.

Verosub, K.L., Mehringer, P.J., Jr & Waterstraat, P., 1986. Holocene secular variation in western North America: paleomagnetic record from Fish Lake, Harney county, Oregon, *J. geophys. Res.,* **91,** 3609–3623.

Wright, H.E., Jr, 1967. A square-rod piston sampler for lake sediments, *J. Sed. Pet.,* **37,** 975–976.

Zijderveld, J.D.A., 1967. AC demagnetization of rocks: analysis of results, in *Methods in Paleomagnetism,* p. 609, eds Collinson, D.W., Creer, K.M. & Runcorn, S.K., Elsevier, Amsterdam.